NEOPLASIA
www.neoplasia.com
Volume 35 Number xxx Month 2023 pp. 100840

Original Research

The kinetics of blast clearance are associated with copy number alterations in childhood B-cell acute lymphoblastic leukemia

Zuzanna Urbańska[a]; Monika Lejman[b]; Joanna Taha[a]; Joanna Madzio[a]; Kinga Ostrowska[a]; Karolina Miarka-Walczyk[a]; Kamila Wypyszczak[a]; Borys Styka[b]; Justyna Jakubowska[a]; Łukasz Sędek[c]; Tomasz Szczepański[c]; Marcin Stańczak[d]; Wojciech Fendler[d,e]; Wojciech Młynarski[a]; Agata Pastorczak[a,*]

[a] Department of Pediatrics, Oncology and Hematology, Medical University of Lodz, Lodz, Poland
[b] Laboratory of Genetic Diagnostics, Medical University of Lublin, Lublin, Poland
[c] Department of Pediatric Hematology and Oncology, Medical University of Silesia, Zabrze, Poland
[d] Department of Biostatistics and Translational Medicine, Medical University of Lodz, Lodz, Poland
[e] Department of Radiation Oncology, Dana-Farber Cancer Institute, Boston, MA, USA

Abstract

We analyzed the pattern of whole-genome copy number alterations (CNAs) and their association with the kinetics of blast clearance during the induction treatment among 195 pediatric patients with B-cell precursor acute lymphoblastic leukemia (BCP-ALL) who displayed intermediate or high levels of minimal residual disease (MRD). Using unsupervised hierarchical clustering of CNAs > 5 Mbp, we dissected three clusters of leukemic samples with distinct kinetics of blast clearance [A – early slow responders (n=105), B – patients with persistent leukemia (n=24), C – fast responders with the low but detectable disease at the end of induction (n=66)] that corresponded with the patients' clinical features, the microdeletion profile,the presence of gene fusions and patients survival. Low incidence of large CNAs and chromosomal numerical aberrations occurred in cluster A which included ALL samples showing recurrent microdeletions within the genes encoding transcription factors (i.e., *IKZF1, PAX5, ETV6*, and *ERG*), DNA repair genes (*XRCC3* and *TOX*), or harboring chromothriptic pattern of CNAs. Low hyperdiploid karyotype with trisomy 8 or hypodiploidy was predominantly observed in cluster B. Whereas cluster C included almost exclusively high-hyperdiploid ALL samples with concomitant mutations in RAS pathway genes. The pattern of CNAs influences the kinetics of leukemic cell clearance and selected aberrations affecting DNA repair genes may contribute to BCP-ALL chemoresistance.

Neoplasia (2023) 35, 100840

Keywords: Acute lymphoblastic leukemia, Children, Chemoresistance, Copy number alterations, Minimal residual disease

Introduction

B-cell precursor acute lymphoblastic leukemia (BCP-ALL) develops as a result of the sequential acquisition of genetic aberrations that block the differentiation of B-cell lymphoid progenitors and maintain the proliferation of leukemic clones. Initiating genetic abnormalities in ALL are aneuploidy (gains and losses of whole chromosomes) and chromosomal translocations leading to the formation of gene fusions, commonly affecting hematopoietic transcription factors, epigenetic modifiers, cytokine receptors, and tyrosine kinases [1]. These primary aberrations directly contribute to the leukemic transformation and define the biology of the main clone. Therefore, they are preferentially used as predictive markers for patient risk stratification. In contrast, secondary abnormalities, including copy number alterations (CNAs) and point mutations promoting leukemia evolution, may be present only in the subset of leukemic cells [2]. However, there is a correlation between the presence of the primary alteration and specific cooperating secondary lesions within genetic subtypes of ALL e.x. *RB1* gene deletions in ALL displaying the intrachromosomal amplification of chromosome 21

* Corresponding author at: Department of Pediatrics, Oncology and Hematology, Medical University of Lodz, Sporna 36/50, 91-738 Lodz, Poland.
E-mail address: agata.pastorczak@umed.lodz.pl (A. Pastorczak).
Received 17 June 2022; accepted 4 October 2022

https://doi.org/10.1016/j.neo.2022.100840

(iAMP21) [3]. In addition, the co-occurrence of CNAs within specific genes may significantly and independently confer a poor prognosis, as was recently described for the microdeletion profile called "*IKZF1*^{plus}" in childhood BCP-ALL [4].

The application of next-generation sequencing provided almost complete insight into the genetic background of ALL [5,6]. However, the biological and clinical heterogeneity of ALL makes direct and rapid application of new genomic markers to personalize adjustment of the primary treatment difficult. Therefore, the assessment of therapy response based on the measurement of minimal residual disease (MRD) is still the most universal and strong single prognostic factor in pediatric ALL [7].

The main advantage of using MRD as a marker of chemoresistance in ALL is that it reflects a combination of effects derived from both host factors and cancer cells [8]. The estimation of the risk of relapse based on serial MRD testing and appropriate adjustments of the intensity of the therapy depending on blast clearance has resulted in the gradual improvement of cure rates in childhood ALL, which now exceed 85% [9]. However, even highly specific and sensitive methodologies for MRD assessment are not able to fully predict ALL relapse [10]. Several factors may modify the prognostic significance of the MRD value, with the most important being: the time point of MRD measurements during therapy, the applied technique of detection, and the genetic subtype of ALL [7]. The level of FC-MRD assessed at day 15 of the induction protocol correlates with the relapse-free survival (RFS) in childhood BCP-ALL, whereas PCR-based MRD predicts relapse when measured at day 33 of the initial therapy [11–14]. Furthermore, the kinetics of blast clearance are strongly modulated by the presence of primary and secondary aberrations [7,15,16]. MRD at the end of induction is log normally but differently distributed among molecular subtypes of ALL and the risk of leukemia recurrence is directly proportional to the MRD level within all genetic subtypes. The fastest kinetics of leukemic cell clearance are observed in *ETV6-RUNX1*- and *TCF3-PBX1*-positive cases. In contrast, patients with the ALL subtype defined as ''B-other'' based on the CNA profile show slower reductions in blast counts over time [7].

In this study, we analyzed the kinetics of blast clearance during the induction phase of the ALL protocol depending on the profile of whole-genome CNAs in patients displaying intermediate or high levels of MRD.

Materials and methods

Study group

We retrospectively analyzed children with newly diagnosed BCP-ALL with an age of 0-18 years treated in the 13 centers of the Polish Pediatric Leukemia/Lymphoma Study Group according to the ALL-IC BFM 2009 and AIEOP-BFM 2017 protocols [17,18]. The inclusion criteria were as follows: bone marrow MRD at day 15 of the treatment protocol exceeding 10% in a flow cytometric measurement and/or bone marrow MRD at day 33 detected by RQ-PCR analysis above 0.001%. Patients diagnosed with secondary leukemia or harboring gene fusions, including *BCR-ABL1, ETV6-RUNX1, TCF3-HLF, TCF3-PBX1, KMT2A-AFF1,* and other *KMT2A* rearrangements, were excluded from the study group. The profile of blast clearance in these molecular subtypes has been extensively investigated [19–24]. The study was conducted in accordance with the Declaration of Helsinki. The research protocol was approved by the Ethics Committee of the Medical University of Lodz, and informed consent was obtained from all participants and/or their parents (No. RNN/228/16/KE).

Minimal residual disease monitoring during the induction phase of the protocols

Bone marrow samples from all BCP-ALL patients at diagnosis and 15. day of the treatment protocol were centrally analyzed by 8-color flow cytometry according to the protocols of the EuroFlow Consortium at one site (Department of Pediatric Hematology and Oncology, Medical University of Silesia in Zabrze) [25]. Bone marrow MRD at the end of the induction phase (day 33) was assessed using RQ-PCR analysis of clone-specific immunoglobulin (*IG*) and T-cell receptor (*TCR*) gene rearrangements according to the guidelines described by van der Velden et al. [26]. MRD analysis detected the presence of at least 10 residual leukemia cells in 1 000 000 cells (10^{-5}).

Microarray analysis

Copy-number variation analysis was performed using the CytoScan HD array (*Applied Biosystems, Thermo Fisher Scientific*, Waltham, MA) and Chromosome Analysis Suite v 4.2 software (ChAS, *Thermo Fisher Scientific*, Waltham, MA). Experimental data were analyzed in two categories: genome-wide CNAs > 5 Mbp and leukemia-associated region/gene-specific CNAs (leukemia genes_all_20150505; Fullerton Overlap Map_hg19). Our panel of n=1276 genes was created based on comprehensive literature describing genetic alterations and their role in the pathogenesis of ALL. The genes are listed in Supplementary Table 1.

RNA sequencing

RNA sequencing was performed using the TruSight RNA Pan-Cancer panel (*Illumina*, San Diego, CA) on a Next Seq 550 system (*Illumina*, San Diego, CA) using NextSeq® Reagent Kit v3 (150 cycles) with a PE NextSeq® Flow Cell. Data analysis was performed using the Illumina BaseSpace apps TopHat Alignment (version 1.0.0, read mapping on hg19 reference genome by TopHat21, fusion calling by TopHat-Fusion2, and RNA-seq Alignment (version 1.1.0, read mapping on hg19 reference genome by STAR3, fusion calling by Manta4 using standard settings (https://basespace.illumina.com/apps). Raw data of sequence variants were analyzed in Variant Studio software v.4.0.

A detailed description of all methods can be found in the online Supplementary materials.

Results

Clinical features of BCP-ALL depending on MRD subgroups

The study enrolled 195 patients with newly diagnosed childhood BCP-ALL who met the inclusion criteria. The cohort was divided into three subgroups depending on levels of MRD at days 15 and 33 of the induction treatment: children with MRD15 ≥ 10% [MRD15], those showing both MRD15 ≥ 10% and MRD33 ≥ 0.001% [MRD15&33], and patients displaying MRD33 ≥ 0.001% [MRD33]. The composition of the analyzed groups is described in a flow diagram (Fig. 1).

Detailed exposure to chemotherapeutics during the induction phase of each protocol is listed in Supplementary Table 2. Patients from both protocols received a similar scheme of a chemotherapy during the first 33 days. The essential difference was associated with the formulation of L-asparaginase (ASP).

Since during the first two weeks of the induction therapy, patients received an increasing dosages of glucocorticoids and only single doses of vincristine, daunorubicin, and ASP, high levels of MRD at day 15 mainly reflect resistance to glucocorticoids. An increased level of MRD at day 33 is associated with the multidrug chemotherapy response. The clinical and biological characteristics of patients treated according to the ALL-IC BFM 2009 and AIEOP-BFM 2017 protocols are presented in Supplementary Table 3.

Patients allocated to the three MRD subgroups significantly differed regarding clinical features (Supplementary Table 4).

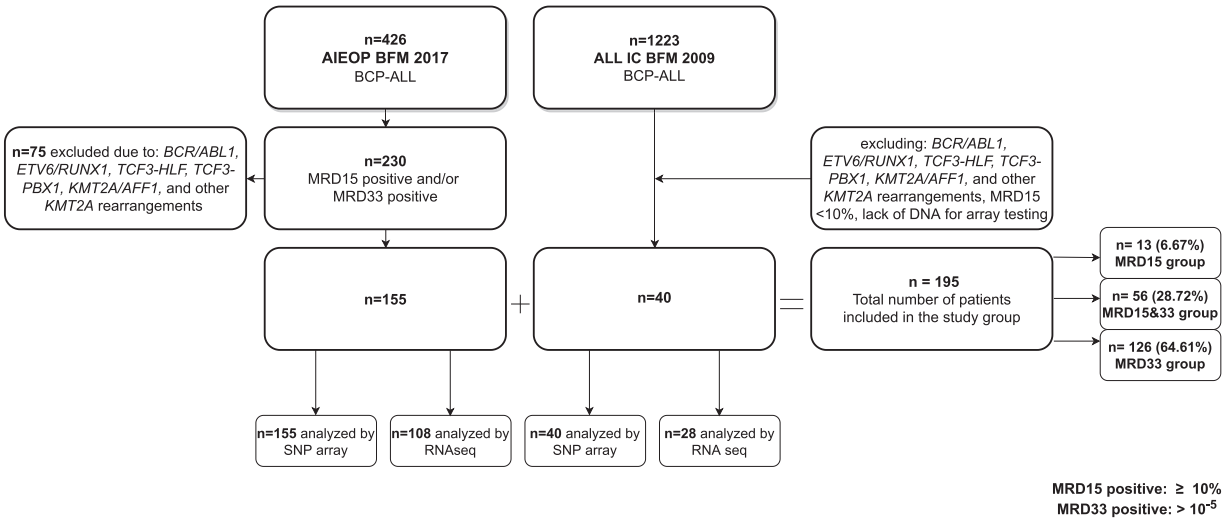

Fig. 1. The algorithm of the study.

Comparison of the cytogenetic and molecular karyotypes of BCP-ALL

Copy-number profiling was reliably performed in all 195 ALL samples (100%) enrolled in the study cohort. Due to the failure of bone marrow cell culture for cytogenetic testing, the results of classical karyotyping were unavailable in 30 out of 195 patients (15.38%). Among 42 out of 165 BCP-ALL samples (25.45%) showing a normal karyotype, 10 cases (23.81%) were also confirmed using an SNP array. Original karyotypes and revisions based on SNP array analysis are presented in Supplementary Table 5. The distribution of CNAs and LOHs exceeding 5 Mbp on particular chromosomes is presented in Supplementary Figure 1.

Numerical chromosomal aberrations depending on MRD subgroups

A hyperdiploid karyotype was identified in n=96 (49.23%) of ALL cases, including low hyperdiploidy (HeL; 47-50 chromosomes) and high hyperdiploidy (HeH; >50 chromosomes) in n=24 (25%) and n=72 (75%) patients, respectively. Overall, a hyperdiploid karyotype was present in 6 out of 13 patients (46.15%) from the MRD15 subgroup, and both HeL and HeH were identified in n=3 (23.08%) cases. In the MRD15&33 subgroup, HeL occurred in n=10 (17.86%) children, while HeH was identified in n=8 (14.29%) patients (total n=56 cases). The highest incidence of hyperdiploidy was seen in the MRD33 subgroup and included n=11 (8.73%) individuals with HeL and n=61 (48.41%) children with HeH (out of 126 total patients). The distribution of hyperdiploidy by modal chromosome number was skewed, with the majority of karyotypes (n=59; 61.46%) showing 8 or more extra chromosomes [modal chromosome number was 54 (range 47-66)]. The pattern of chromosome gain was nonrandom, with chromosomes X, 21, 14, 4, 6, and 18 being the most frequently gained. The majority of the gains were trisomies, but tetrasomies were also detected for chromosomes 21 (n=43; 44.79% of the 96 cases), 14 (n=12; 12.5%), X (n=5; 11.11% of 45 girls), 4 (n=3; 3.12%), and 18 (n=3; 3.12%). Interestingly, chromosome loss occurred in 5/195 (2.56%) patients. Again, the pattern of loss appeared nonrandom, with chromosome 7 being lost most commonly, followed by single cases displaying monosomy of chromosomes 9, 13, 15, or 20.

SNP array revealed a near-haploid karyotype in n=5 (2.56%) ALL cases with hypodiploid clones containing 28-31 chromosomes in all but one patient. Two of them (M29 and M195; Supplementary Table 5), initially classified as HeH by cytogenetics, were masked hypodiploidy. The ALL cases with near-haploidy were most likely to remain disomic for chromosomes 14, 18, 21, and X/Y.

The distribution of large structural aberrations >5 Mbp within MRD subgroups

We investigated whether MRD subgroups showed different frequencies and diverse spectra of structural aberrations exceeding 5 Mbp. In the case of duplications, after correction for multiple comparisons, the only significant difference resulted from the more frequent incidence of whole chromosomal gains involving chromosomes X, 17, 14, 10, 6, and 4 in the MRD33 subgroup than in the MRD15 and MRD15&33 subgroups (Fig. 2A). Similarly, although the frequency and spectrum of large deletions affecting chromosomes 20q, 9q, and 6q differed between MRD subgroups ($p<0.05$), no significant results for specific alterations were obtained with FDR<0.05 (Fig. 2B). In the next step of the analysis, we performed unsupervised hierarchical clustering, which allowed the classification of 195 ALL samples based on their similarities regarding the incidence of CNA > 5 Mbp. A clear separation into three clusters exhibiting a significantly distinct response to the treatment was identified (Fig. 2C).

Cluster A contained 105 patients who showed a high level of MRD at day 15 and low positive MRD at day 33 of the induction protocol, we called them ''early slow responders''. Patients with "persistent leukemia" (n=24 ALL cases), who were more likely to display both increased levels of MRD at day15. and 33., were assigned to cluster B. Whereas those allocated to cluster C (n=66 patients) were early fast responders with predominantly low but positive MRD at the end of the induction protocol (Fig. 3).

The clinical characteristics of patients significantly differed depending on the cluster (Table 1.).

We observed the trend of different overall survival (OS) between clusters within short median follow-up time of 10.87 (7.37-15.73) months. OS for Cluster A, B, and C were as follows 0.75, 0.85 and 0.9, respetively (p=0.067) (Supplementary Figure 2.). The probablilty of relapse free survival (RFS) did not statistically differed depending on the cluster, however any relapse occured in cluster C during the follow-up time.

In the karyotype of one-third of ALL samples classified as cluster A (n=32/105; 30.48%), no large CNAs were observed. In addition, in this group of patients, HeH was completely absent, whereas HeL occurred in 10 patients (9.52%). In this group, the recurrent interstitial gain was found on a long arm of chromosome 1, which encompassed the common 1q23.3q44 (164786865_249224684) region. However, copy number losses definitely dominated in the cluster A, with the most frequent deletions affecting chromosomes 9 (n=27; 25.71%), 7 (n=13; 12.38%), 12 (n=12; 11.43%) and 20 (n=8; 7.62%). Copy number losses

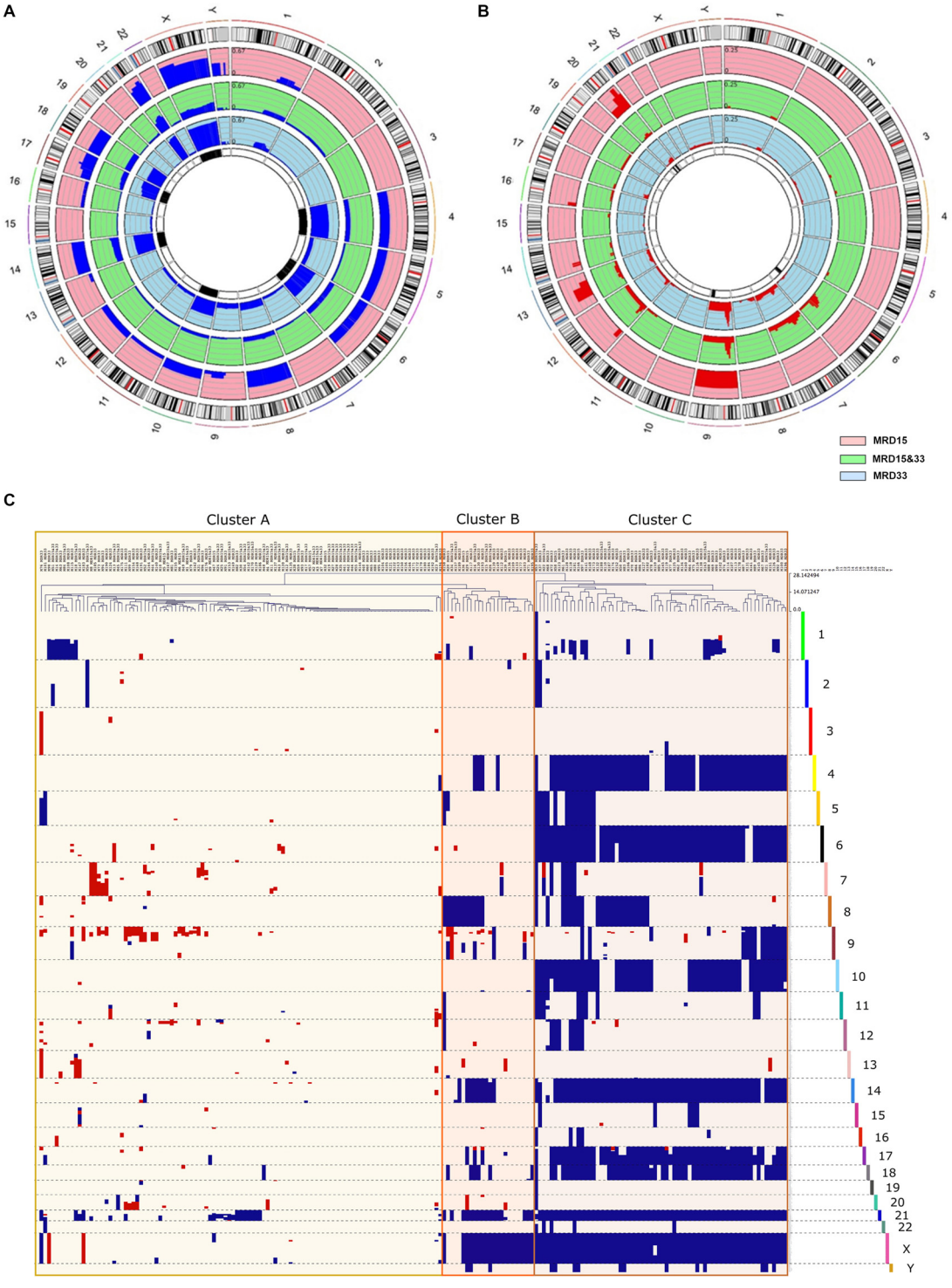

Fig. 2. Histograms displaying the frequency of gains (A) and losses (B) exceeding 5 Mbp in the study group depending on the MRD group. (C) Hierarchical clustering analysis based on CNAs data obtained from 195 pediatric BCP-ALL samples.

located on the short arm of chromosome 9 predominantly involved the 9p21.3p13.2 (21197288_36892411) region, which includes *CDKN2A/B, FANCG,* and *PAX5* genes. Large structural aberrations of chromosome 7 included two monosomies, nine 7q deletions encompassing a common 7q33q35 (134698398_143838984) region and eight 7p deletions involving 7p13p12.2 (43433655_50434024) region containing *HUS1* and *IKZF1* genes. The most commonly deleted chromosomal region on chromosome 12 was located at the short arm 12p13.2p13.1 (11361150_13625042) and encompassed *ETV6, BCL2L14,* and *CDKN1B* genes. Five out of eight large losses on chromosome 20 affected the whole long arm of chromosome 20, and two of them led to the formation of the chromosome abnormality dic(9;20)(p13;q11.2), as confirmed by karyotype and FISH analyzes.

Half of the ALL cases classified into cluster B (n=12) showed a low hyperdiploid karyotype (HeL) with a relatively frequent incidence of

Table 1

Clinical characteristics of patients depending on the cluster of large aberrations >5Mbp.

	Cluster A	Cluster B	Cluster C	*P value*	Post-hoc *p value*
Sex, n(%)					
Male	61 (58.1%)	10 (41.67%)	37 (56.06%)	**0.34**[a]	
Female	44 (41.9%)	14 (58.33%)	29 (43.94%)		
Age (years)					
Median	8.27 (4.4-11.8)	5.94 (4.02-8.58)	3.99 (2.95-5.72)	**$<10^{-4}$**[b]	**2×10^{-5}****
<1	5	0	1		
1-9	58	20	57		
10-14	28	4	7		
15-18	14	0	1		
WBC (10^6/L)					
Median	11700 (4020-74985)	4760 (2012-20700)	8010 (3600-24700)	**0.025**[b]	**0.406**
Unknown/ Missing	5	1	0		
CNS involvement					
CNS1	87 (82.85%)	19 (79.16%)	55 (83.33%)	**0.85**[a]	
CNS2	7 (6.67%)	3 (12.5%)	7 (10.61%)		
CNS3	7 (6.67%)	1 (4.17%)	4 (6.06%)		
Unknown/ Missing	4 (3.81%)	1 (4.17%)	0		
Steroidoresistance n (%)					
Yes	19 (18.09%)	1 (4.17%)	4 (6.06%)	**0.017**[a]	
Not	74 (70.48%)	21 (87.5%)	59 (89.39%)		
Unknown/ Missing	12 (11.43%)	2 (8.33%)	3 (4.55%)		
Risk group					
SRG	0	0	1	**10^{-4}**[a]	
IRG	33	11	49		
HRG	53	11	12		
Unknown/ Missing	18	2	4		
CR achieved					
Yes	83	20	62	**0.57**[a]	
No	3	0	1		
Unknown/ Missing	19	4	3		
FCM MRD 15 (%)					
Median	8.19 (0.82-23.90)	5.43 (0.21-17.17)	0.77 (0.15-4.63)	**0.0002**[b]	**< 0.0001****
PCR MRD 33 (%)					
Median	0.05 (0.01-0.59)	0.16 (0.01-0.60)	0.01 (0.01-0.06)	**0.0021**[b]	**0.0019****
Number of patients assigned to MRD group					
MRD15	6 (5.71%)	4 (16.67%)	3 (4.55%)	<	
MRD15&33	44 (41.90%)	5 (20.83%)	7 (10.61%)	**0.0001**	
MRD33	55 (52.38%)	15 (62.50%)	56 (84.85%)		
Total n (%)	105 (53.84%)	24 (12.31%)	66 (33.85%)		

[a] *Chi^2 test*

[b] *ANOVA Kruskall-Wallis.* ANOVA Kruskall-Wallis test with post-hoc p-value for comparison between Cluster A and Cluster B was marked with one asterix (*), between Cluster A and Cluster C groups with two asterix (**), between Cluster B and Cluster C with three asterix (***). Abbreviations: WBC-white cell blood count, BM-bone marrow, SRG-standard risk group, IRG-intermediate risk group, HRG-high risk group.

trisomy of chromosome 8 (n=5; 41.66%). Interestingly, all five hypodiploid leukemias were also assigned to this cluster.

Cluster C included almost exclusively HeH cases with frequent (n=16/66; 24.24%) cooccurring duplications that affected the long arm of chromosome 1. The commonly gained region was located within the chromosomal 1q21.2q32.1(149850339_205768488) region and included 49 genes from cytoregions.

The profile of microdeletions and microduplications < 5 Mbp in the MRD subgroups

We further studied the profile of microaberrations involving coding regions of 1276 genes showing a proven connection with the leukemia development and/or outcome (Supplementary Figure 3). Overall, we found n=459 microdeletions and n=173 microduplications within the cytoregions in 149 and 76 patients, respectively, their mean numbers per ALL sample were 2.35 and 0.89. The frequencies of gene losses per sample in the cluster A, cluster B, and cluster C subgroups were 3.11, 2.7, and 1.01, respectively (p=0.0001). The highest but insignificant incidence of gains was found in cluster B (1.25 versus 0.88 in cluster A and 0.76 in cluster C; p=0.608). There was a significant overrepresentation of microaberrations within genes encoding signaling pathways regulators (p=0.009), cell cycle regulators (p=0.011), and lymphocyte specific genes (p=0.002) in cluster A (Supplementary Figure 4).

The most recurrent lesions affected genes encoding transcription factors, including *IKZF1* (n=32; 16.4%), *PAX5* (n=18; 9.2%), *ETV6* (n=11; 5.6%), and *ERG* (n=11; 5.6%). These aberrations were not equally distributed, but all of them dominated in cluster A. Recurrent deletions also occurred in genes regulating the ALL response to glucocorticoids, including *BTG1* (n=8; 4.1%), *TBL1XR1* (n=5; 2.6%), *CD200* (n=5; 2.6%) and *BTLA* (n=6; 3.1%). Although alterations of these genes were rare, they exclusively affected patients assigned to cluster A, similarly as microdeletions

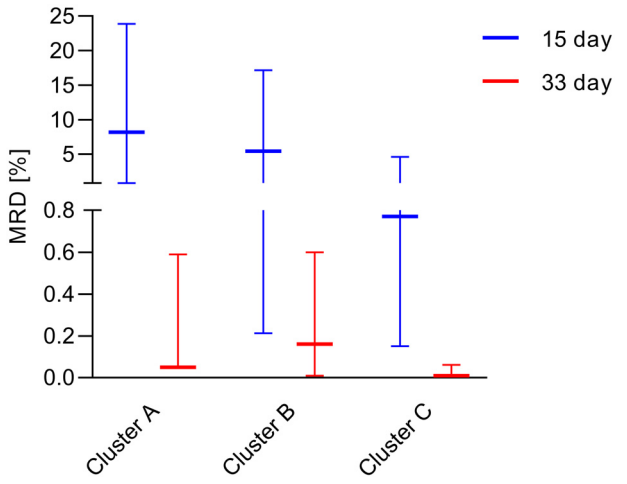

Fig. 3. The levels of minimal residual disease (MRD) at day 15 and at day 33 of induction treatment depending on the CNAs cluster. The vertical line represents median MRD value and the whiskers show the upper and the lower quartile.

within DNA repair genes, such as *XRCC3* (n=7; 3.6%) and *TOX* (n=7; 3.6%).

Gene fusions and sequence mutations across the MRD subgroups

To investigate the frequency of specific gene fusions and gene mutations in the study group, we performed targeted RNA sequencing in 136 out of 195 patients (69.74%) with available RNA from ALL diagnosis. In-frame gene fusions were identified in 20/136 patients (14.7%), including n=18 individuals assigned to cluster A (Supplementary Table 6). *PAX5* and *ZNF384* were the most frequently rearranged genes.

The most recurrent point mutations affected RAS pathway genes and were observed in 49/195 (25%) BCP-ALL patients. Most abnormalities were activating mutations in *NRAS* (48%) and *KRAS* (28%), followed by mutations in *PTPN11* and *FLT3* (11% and 8%, respectively). (Supplementary Figure 5. A). Pathogenic variants in *KRAS* (Supplementary Figure 5. B) and *NRAS* (Supplementary Figure 5. C) were predominantly located within codons 12 and 13. The majority co-occurred with a high hyperdiploid karyotype (n=28/49; 57.14%) and was classified to cluster C (26/49; 53.06%).

Five patients harbored pathogenic activating *JAK2* mutations: c.2047A>G, p. Arg683Gly and c.2624C>A, p. Thr875Asn affecting the *JAK2* pseudokinase and kinase domain, respectively. All but one sample were assigned to cluster A.

Sequencing and microarray studies allowed us to better define the structure of the study group according to the molecular subtype (Supplementary Figure 6.).

The incidence of "chromothriptic-like" phenomenon

Although microarrays have limited ability to distinguish chromothripsis events from progressive DNA alterations in the cancer genome, using criteria for this inference provided by Korbel J and Campbell P [27], we identified chromothriptic-like phenomena in three BCP-ALL cases (Fig. 4).

In each of them, we observed more than ten segmental copy number oscillations that clustered along the chromosome arm, with only one to two (occasionally three) copy number states being interspersed with regions displaying disomic copy number. In addition, the chromosomal regions in the disomic copy-number state retained a heterozygosity. The chromothriptic pattern of CNAs was exclusively observed in patients assigned to the cluster A, MRD33 subgroup and occurred on the long arm of chromosomes 7 and 17, as well as, on a short arm of chromosome 19. Analysis of somatic alterations in BCP-ALL samples suspected of chromothripsis revealed the presence of molecular defects within essential tumor suppressor genes (Supplementary Table 7). One patient showed monoallelic loss of the whole *RB1* gene. Two individuals harbored *TP53* alterations, including whole gene deletion and pathogenic sequence mutation c.701G>A, p. Arg273His that affects the DNA binding domain.

Discussion

CNAs represent cooperating lesions involved in the development of BCP-ALL that may be acquired or lost during disease progression [2]. Both primary and secondary genetic abnormalities may influence the kinetics of blast clearance and therefore strongly predict outcome in ALL [7]. In this study, we retrospectively analyzed whole genome CNAs in pediatric patients with BCP-ALL displaying high or intermediate levels of MRD during the induction phase of therapy.

Since day 15 was the first time point of MRD analysis during the induction protocol, its level mainly reflects sensitivity to glucocorticoids. The vast majority of patients with FC MRD15 ≥10% showed a concomitant positive level of MRD at day 33 (81.16%). These patients were predominantly assigned to cluster A or B, which means that many of them carried copy number losses affecting chromosomes 9, 7, 12, and 20. One of the interesting findings among ALL cases classified into cluster A was a recurrent interstitial gain of 1q that occurred outside of the hyperdiploid karyotype. The minimally gained segment of chromosome 1q in our cohort corresponds with the size and location of duplication reported in the literature in HeH ALL (1q22-32.3) [28]. Gain of 1q leads to overexpression of genes located within the duplicated chromosomal region, including *DAP3* and *UCK2,* that strongly affect cancer development and progression, but their role in the ALL response to treatment has not been examined [28–30].

The overall number of microdeletions was the highest in cluster A compared to the remaining groups. Both large copy number losses and microdeletions frequently comprised regions encoding B-lineage transcription factors that are involved in lymphoid maturation and differentiation (*IKZF1, PAX5, EBF1*, and *ETV6*) as well as cell cycle regulators and tumor suppressors (*CDKN2A/B, BTG1, RB1*), regulators of lymphoid signalling (*BTLA* and *CD200*), and chromatin modifiers (*TBL1XR1*). Our observations are then consistent with previous studies reporting prognostic significance of the CNA profile within these genes among BCP-ALL patients showing intermediate-risk cytogenetics [31]. However, in the cited study, the predictive value of the CNA profile was still, to some extent, modulated by levels of MRD, indicating that the specific configuration of microdeletions influenced leukemic cell chemosensitivity. The most prominent example confirming this thesis is genetic aberrations within *IKZF1* that impair the glucocorticoid response and therefore are related to slow blast clearance during induction treatment [4,15].

Regarding the incidence of gene rearrangements, kinase activating fusions were overrepresented among patients displaying the highest MRD at both time points, which is consistent with observations from previous studies documenting poor response to the induction therapy in patients with the *BCR-ABL1*-like ALL [7,20,32]. In our study group, individuals carrying *PDGFRB* rearrangements showed the slowest blast clearance. Therefore, these individuals could probably benefit from targeted therapy with tyrosine kinase inhibitors.

The majority of ALL patients from our cohort (64.62%) showed selectively positive MRD at day 33, which was associated with multidrug chemotherapy resistance. These patients were assigned to cluster C. The clear predominance of a high hyperdiploid karyotype with coexisting RAS pathway mutations was observed in these individuals. According to the study

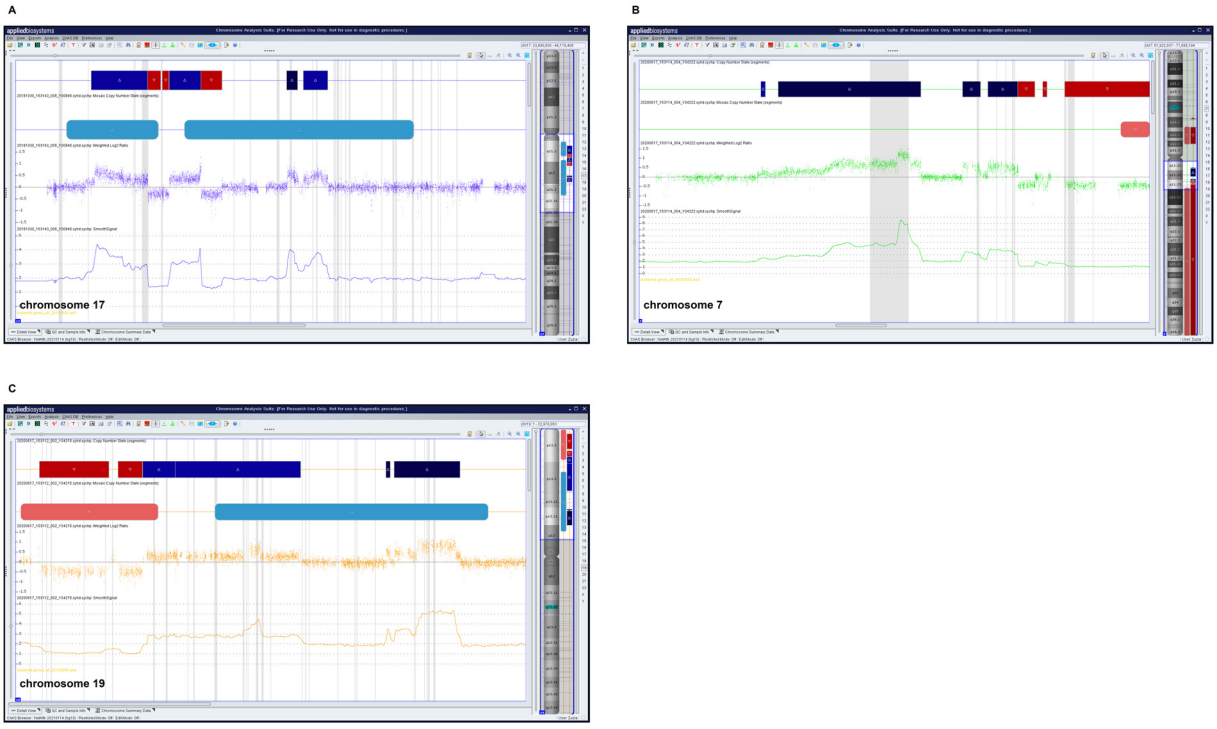

Fig. 4. The incidence of the chromothripsis among BCP-ALL samples: at a long arm of chromosome 17 (A), at a long arm of chromosome 7 (B), and at a short arm chromosome 19 (C).

performed by Jerchel I. et al., clonal RAS pathway activating mutations are present in 24.1% of BCP-ALL and cooccur with several primary aberrations, including the most common high hyperdiploidy [33]. Leukemic blasts carrying RAS mutations are *ex vivo* resistant to prednisolone and vincristine, which probably contribute to an increased level of MRD at the end of induction [33,34]. This group of patients showed the most favourable outcome and low risk of early relapse.

We observed interesting recurrent molecular aberrations involving DNA repair genes, including loss of the whole *XRCC3* gene and deletion of exon 1 of the *TOX* gene, that were exclusively seen in patients with positive MRD at the end of induction treatment. Both genes maintain chromosome stability, but their inactivation has not been investigated in BCP-ALL [35,36,37]. However, in all of the ALL samples, we observed recurrent deletions of exon 1 of the *TOX* gene, which probably results in low gene expression and impaired protein function if only rearrangements involving *TOX* occurred. Since the breakpoint within intron 1 is located in the low complexity region of the gene upstream of the SMART domain (HMG), possible fusion involving the 3' end of the *TOX* gene could lead to gain of gene function with all similar functional consequences that have been described in T-ALL [37].

Another compelling finding in cluster A was the presence of somatic aberrations affecting essential tumor suppressor genes such as *TP53* and *RB1* coexisting with the ''chromothriptic-like'' phenomenon. Chromothripsis is a one-step catastrophic genomic event leading to tens to hundreds of locally clustered DNA rearrangements interspersed with losses of sequence fragments which is perceived as a driver of both cancer development and progression [27,38]. It occurs in 2%-3% of malignancies, but its frequency varies between tumor entities, with BCP-ALL being rarely affected [38,39]. Chromothripsis has been reported in patients with medulloblastoma carrying germline *TP53* mutations or biallelic *BRCA2* mutations [40,41]. Somatic inactivation of *RB1* and *TP53* has been noted in leiomyosarcomas exhibiting chromothripsis [42], suggesting that both germline and somatic aberrations within DNA repair genes may increase the risk of chromothripsis [43].

One of the main limitations of our study results from the short follow-up. Therefore, in the analysis of the influence of detected CNAs on patient survival and incidence of relapse we could only address the risk of early death and early leukemia recurrence. Additionally, targeted RNA sequencing did not allow for sensitive detection of many subclonal point mutations that could affect the response to treatment.

In conclusion, our study adds to the body of evidence that supports the influence of secondary abnormalities on the kinetics of leukemic cell clearance and indicates the possible role of aberrations affecting DNA repair genes in promoting ALL chemoresistance.

Funding

A.P. and Z.U. were supported by the Polpharma Scientific Foundation, grant No. 9/XV/16. W.M., A.P., Z.U. and K.O. were supported by the Team-Net program (POIR.04.04.00-00-16ED/18-00) of the Foundation for Polish Science co-financed by the European Union under the European Regional Development Fund. L.S., W.M. and T.S. were supported by STRATEGMED3/304586/5/NCBR/2017 Person ALL grant of the Polish National Center for Research and Development and internal Medical University of Silesia Grants.

Author contributions

Agata Pastorczak: conceptualization, methodology, formal analysis, writing - review & editing, project administration, Zuzanna Urbańska: conceptualization, data curation, investigation, formal analysis, writing - original draft, Monika Lejman: formal analysis, Joanna Taha: investigation, resources, Joanna Madzio, Kinga Ostrowska, Karolina Miarka-Walczyk, Borys Styka, Łukasz Sędek, Tomasz Szczepański: investigation, Justyna Jakubowska: resources, Marcin Stańczak and Wojciech Fendler: validation and visualization, Wojciech Młynarski: conceptualization, supervision.

Declaration of Competing Interest

The authors declare no conflicts of interest. The funders had no role in the design of the study; in the collection, analyses, or interpretation of data; in the writing of the manuscript; or in the decision to publish the results.

Supplementary materials

Supplementary material associated with this article can be found, in the online version, at doi:10.1016/j.neo.2022.100840.

References

[1] Roberts KG. Genetics and prognosis of ALL in children vs adults. *Hematology* 2018;**2018**(1):137–45. doi:10.1182/asheducation-2018.1.137.

[2] Moorman AV. New and emerging prognostic and predictive genetic biomarkers in B-cell precursor acute lymphoblastic leukemia. *Haematologica* 2016;**101**(4):407–16. doi:10.3324/haematol.2015.141101.

[3] Schwab CJ, Chilton L, Morrison H, et al. Genes commonly deleted in childhood B-cell precursor acute lymphoblastic leukemia: Association with cytogenetics and clinical features. *Haematologica* 2013;**98**(7):1081–8. doi:10.3324/haematol.2013.085175.

[4] Stanulla M, Dagdan E, Zaliova M, et al. IKZF1 plus defines a new minimal residual disease-dependent very-poor prognostic profile in pediatric b-cell precursor acute lymphoblastic leukemia. *J Clin Oncol* 2018;**36**(12):1240–9. doi:10.1200/JCO.2017.74.3617.

[5] Zaliova M, Stuchly J, Winkowska L, et al. Genomic landscape of pediatric B-other acute lymphoblastic leukemia in a consecutive European cohort. *Haematologica* 2019;**104**(7):1396–406. doi:10.3324/haematol.2018.204974.

[6] Kimura S, Mullighan CG. Molecular markers in ALL: Clinical implications. *Best Pract Res Clin Haematol* 2020;**33**(3). doi:10.1016/j.beha.2020.101193.

[7] O'Connor D, Enshaei A, Bartram J, et al. Genotype-Specific minimal residual disease interpretation improves stratification in pediatric acute lymphoblastic leukemia. *J Clin Oncol* 2018;**36**(1):34–43. doi:10.1200/JCO.2017.74.0449.

[8] Campana D. Minimal residual disease monitoring in childhood acute lymphoblastic leukemia. *Curr Opin Hematol* 2012;**19**(4):313–18. doi:10.1097/MOH.0b013e3283543d5c.

[9] Pieters R, De Groot-Kruseman H, Van Der Velden V, et al. Successful therapy reduction and intensification for childhood acute lymphoblastic leukemia based on minimal residual disease monitoring: Study ALL10 from the Dutch Childhood Oncology Group. *J Clin Oncol* 2016;**34**(22):2591–601. doi:10.1200/JCO.2015.64.6364.

[10] Kruse A, Abdel-Azim N, Kim HN, et al. Minimal residual disease detection in acute lymphoblastic leukemia. *Int J Mol Sci* 2020;**21**(3). doi:10.3390/ijms21031054.

[11] Basso G, Veltroni M, Valsecchi MG, et al. Risk of relapse of childhood acute lymphoblastic leukemia is predicted by flow cytometric measurement of residual disease on day 15 bone marrow. *J Clin Oncol* 2009;**27**(31):5168–74. doi:10.1200/JCO.2008.20.8934.

[12] Zawitkowska J, Lejman M, Romiszewski M, et al. Results of two consecutive treatment protocols in Polish children with acute lymphoblastic leukemia. *Sci Rep* 2020;**10**(1). doi:10.1038/s41598-020-75860-6.

[13] Kim IS. Minimal residual disease in acute lymphoblastic leukemia: technical aspects and implications for clinical interpretation. *Blood Res* 2020;**55**(S1):19–26. doi:10.5045/br.2020.S004.

[14] van der Velden VHJ, Panzer-Grümayer ER, Cazzaniga G, et al. Optimization of PCR-based minimal residual disease diagnostics for childhood acute lymphoblastic leukemia in a multi-center setting. *Leukemia* 2007;**21**(4):706–13. doi:10.1038/sj.leu.2404535.

[15] Marke R, Havinga J, Cloos J, et al. Tumor suppressor IKZF1 mediates glucocorticoid resistance in B-cell precursor acute lymphoblastic leukemia. *Leukemia* 2016;**30**(7):1599–603. doi:10.1038/leu.2015.359.

[16] Braun M, Pastorczak A, Fendler W, et al. Biallelic loss of CDKN2A is associated with poor response to treatment in pediatric acute lymphoblastic leukemia. *Leuk Lymphoma* 2017;**58**(5):1162–71. doi:10.1080/10428194.2016.1228925.

[17] A Randomized Trial of the I-BFM-SG for the Management of Childhood - B Acute Lymphoblastic Leukemia, Published, 2009. http://www.bialaczka.org/wp-content/uploads/2016/10/ALLIC_BFM_2009.pdf.

[18] Treatment Protocol for Children and Adolescents With Acute Lymphoblastic Leukemia - AIEOP-BFM ALL 2017. https://clinicaltrials.gov/ct2/show/NCT03643276

[19] Leoni V, Biondi A. Tyrosine kinase inhibitors in BCR-ABL positive acute lymphoblastic leukemia. *Haematologica* 2015;**100**(3):295. doi:10.3324/HAEMATOL.2015.124016.

[20] Boer JM, Steeghs EMP, Marchante JRM, et al. Tyrosine kinase fusion genes in pediatric BCR-ABL1-like acute lymphoblastic leukemia. *Oncotarget* 2017;**8**(3):4618–28. doi:10.18632/oncotarget.13492.

[21] Bhojwani D, Pei D, Sandlund JT, et al. ETV6-RUNX1-positive childhood acute lymphoblastic leukemia: improved outcome with contemporary therapy. *Leuk 2012 262* 2011;**26**(2):265–70. doi:10.1038/leu.2011.227.

[22] Fischer U, Forster M, Rinaldi A, et al. Genomics and drug profiling of fatal TCF3-HLF-positive acute lymphoblastic leukemia identifies recurrent mutation patterns and therapeutic options. *Nat Genet* 2015;**47**(9):1020. doi:10.1038/NG.3362.

[23] Felice MS, Gallego MS, Alonso CN, et al. Prognostic impact of t(1;19)/TCF3-PBX1 in childhood acute lymphoblastic leukemia in the context of Berlin-Frankfurt-Münster-based protocols. *Leuk Lymphoma* 2011;**52**(7):1215–21. doi:10.3109/10428194.2011.565436.

[24] Forgione MO, McClure BJ, Eadie LN, Yeung DT, White DL. KMT2A rearranged acute lymphoblastic leukaemia: Unravelling the genomic complexity and heterogeneity of this high-risk disease. *Cancer Lett* 2020:469. doi:10.1016/J.CANLET.2019.11.005.

[25] Kalina T, Flores-Montero J, Van Der Velden VHJ, et al. EuroFlow standardization of flow cytometer instrument settings and immunophenotyping protocols. *Leukemia* 2012;**26**(9):1986–2010. doi:10.1038/leu.2012.122.

[26] van der Velden VHJ, Cazzaniga G, Schrauder A, et al. Analysis of minimal residual disease by Ig/TCR gene rearrangements: Guidelines for interpretation of real-time quantitative PCR data. *Leukemia* 2007;**21**(4):604–11. doi:10.1038/sj.leu.2404586.

[27] Korbel JO, Campbell PJ. Criteria for inference of chromothripsis in cancer genomes. *Cell* 2013;**152**(6):1226–36. doi:10.1016/j.cell.2013.02.023.

[28] Davidsson J, Andersson A, Paulsson K, et al. Tiling resolution array comparative genomic hybridization, expression and methylation analyses of dup(1q) in Burkitt lymphomas and pediatric high hyperdiploid acute lymphoblastic leukemias reveal clustered near-centromeric breakpoints and overexpression o. *Hum Mol Genet* 2007;**16**(18):2215–25. doi:10.1093/hmg/ddm173.

[29] Han J, An O, Hong HQ, et al. Suppression of adenosine-to-inosine (A-to-I) RNA editome by death associated protein 3 (DAP3) promotes cancer progression. *Sci Adv* 2020;**6**(25). doi:10.1126/sciadv.aba5136.

[30] Wu Y, Jamal M, Xie T, et al. Uridine-cytidine kinase 2 (UCK2): a potential diagnostic and prognostic biomarker for lung cancer. *Cancer Sci* 2019;**110**(9):2734–47. doi:10.1111/cas.14125.

[31] Hamadeh L, Enshaei A, Schwab C, et al. Validation of the United Kingdom copy-number alteration classifier in 3239 children with B-cell precursor ALL. *Blood Adv* 2019;**3**(2):148–57. doi:10.1182/bloodadvances.2018025718.

[32] Roberts KG, Pei D, Campana D, et al. Outcomes of children with BCR-ABL1-like acute lymphoblastic leukemia treated with risk-directed therapy based on the levels of minimal residual disease. *J Clin Oncol* 2014;**32**(27):3012–20. doi:10.1200/JCO.2014.55.4105.

[33] Jerchel IS, Hoogkamer AQ, Ariës IM, et al. RAS pathway mutations as a predictive biomarker for treatment adaptation in pediatric B-cell precursor acute lymphoblastic leukemia. *Leukemia* 2018;**32**(4):931–40. doi:10.1038/leu.2017.303.

[34] Ariës IM, van den Dungen RE, Koudijs MJ, et al. Towards personalized therapy in pediatric acute lymphoblastic leukemia: RAS mutations and prednisolone

resistance. *Haematologica* 2015;**100**(4):e132–6. doi:10.3324/haematol.2014.112995.

[35] Pierce AJ, Johnson RD, Thompson LH, Jasin M. XRCC3 promotes homology-directed repair of DNA damage in mammalian cells. *Genes Dev* 1999;**13**(20):2633–8. doi:10.1101/gad.13.20.2633.

[36] Osti MF, Nicosia L, Agolli L, et al. Potential Role of Single Nucleotide Polymorphisms of XRCC1, XRCC3, and RAD51 in Predicting Acute Toxicity in Rectal Cancer Patients Treated with Preoperative Radiochemotherapy. *Am J Clin Oncol Cancer Clin Trials* 2017;**40**(6):535–42. doi:10.1097/COC.0000000000000182.

[37] Lobbardi R, Pinder J, Martinez-Pastor B, et al. TOX regulates growth, DNA repair, and genomic instability in T-cell acute lymphoblastic leukemia. *Cancer Discov* 2017;**7**(11):1336–53. doi:10.1158/2159-8290.CD-17-0267.

[38] Stephens PJ, Greenman CD, Fu B, et al. Massive genomic rearrangement acquired in a single catastrophic event during cancer development. *Cell* 2011;**144**(1):27–40. doi:10.1016/j.cell.2010.11.055.

[39] Voronina N, Wong JKL, Hübschmann D, et al. The landscape of chromothripsis across adult cancer types. *Nat Commun* 2020;**11**(1). doi:10.1038/s41467-020-16134-7.

[40] Rausch T, Jones DTW, Zapatka M, et al. Genome sequencing of pediatric medulloblastoma links catastrophic DNA rearrangements with TP53 mutations. *Cell* 2012;**148**(1-2):59–71. doi:10.1016/j.cell.2011.12.013.

[41] Ratnaparkhe M, Wong JKL, Wei PC, et al. Defective DNA damage repair leads to frequent catastrophic genomic events in murine and human tumors. *Nat Commun* 2018;**9**(1). doi:10.1038/s41467-018-06925-4.

[42] Chudasama P, Mughal SS, Sanders MA, et al. Integrative genomic and transcriptomic analysis of leiomyosarcoma. *Nat Commun* 2018;**9**(1). doi:10.1038/s41467-017-02602-0.

[43] Ratnaparkhe M, Hlevnjak M, Kolb T, et al. Genomic profiling of Acute lymphoblastic leukemia in ataxia telangiectasia patients reveals tight link between ATM mutations and chromothripsis. *Leukemia* 2017;**31**(10):2048–56. doi:10.1038/leu.2017.55.